第14章 大動脈瘤

A. 胸部大動脈瘤

竹谷　剛，髙本眞一

本邦における胸部大動脈瘤手術は1980年代後半に年間1,200件程度であったものが2006年には9,300件を超えるまでに増加した[1]。原因としては診断技術の進歩や診断機会の増加，手術の安全性向上による手術適応の拡大，生活習慣の欧米化や人口の高齢化による動脈硬化人口の増加など様々な因子が挙げられる。2006年には真性動脈瘤に対する手術はこのうち5,000件程度であったが，etiologyとしては動脈硬化が大部分を占めており，Marfan症候群に代表される結合織疾患がこれに続く。高安動脈炎やベーチェット病などの動脈炎によるものは，動脈瘤を形成するに至るまでの診断や治療法の進歩により減少し，梅毒性中膜炎に起因するものも治療法の進歩や梅毒自体の減少により稀なものとなりつつある。

1. 診断

CT(特に造影CT)が診断のgold standardである。CTの発達した今日では血管造影の有用性はほとんどない。

2. 予後と手術適応

胸部大動脈瘤は自覚症状に乏しい疾患であり，治療は破裂による突然死と，解離の発生に伴う様々な合併症を予防するために施行される。

日本循環器学会の大動脈瘤・大動脈解離診療ガイドライン[2]による胸部大動脈瘤手術適応は，最大短径 60mmを超えるものがClass I とされており，欧米でも60mmが一般的な手術適応とされる。これは，瘤径60mmを超えると破裂や解離，死亡のリスクが指数関数的な増大を示すためで，60mmを超える瘤は年間15.6%に破裂，解離を発生，もしくは死亡するとされる[3]。欧米人に比べ日本人の体格が比較的小さいことと，手術成績も本邦のほうが概ね良好なことから，大きな手術リスクのない患者であれば55～60mmを手術のタイミングとすることが多いようであるが，瘤の形状や拡大速度，併存症の有無等の手術リスクにより患者個々にとって手術適応径は異なってしかるべきである。また結合織疾患の有無や解離発症の既往，解離や破裂の家族歴も重要で，大動脈解離の既往のあるMarfan症候群の大動脈弁輪拡張症に対しては40～45mmを手術適応とすることもある。

3. 外科治療

人工心肺を用いた人工血管置換術が依然gold standardである。弓部大動脈瘤においては脳保護，下行大動脈瘤においては脊髄梗塞の予防が特に重要となる。また，大動脈弁輪拡張症に対しては従来composite graftを用いたBentall型手術が一般的であったが，弁尖に変性のない多くの症例に対しては自己弁温存術式(Reimplantation法：David手術，Remodeling法：Yacoub手術)が近年行われるようになり，良好な中・遠隔期成績が報告されている[4,5]。

また，open surgeryに代わる方法としては，2008年７月に胸部大動脈瘤治療用の企業製ステントグラフトが保険収載されたこともあり，今後ステントグラフトによる治療が増加してゆくものと考えられる。局所麻酔でも施行可能であり，全身麻酔下の開胸・開腹手術が高リスクとなる患者にとってメリットは大きい。

手術成績は年々向上しており，日本胸部外科学会の2006年の統計では，胸部大動脈手術overallの在院死亡率は10.5%，待機的な弓部大動脈置換では6.5%，下行大動脈置換は5.8%，急性大動脈解離に対する上行大動脈置換で12.9%であった[1]。

4. 内科治療

アンジオテンシンII受容体拮抗薬，ACE阻害薬，スタチン，テトラサイクリン系抗生物質，マクロライド系抗生物質，βブロッカー等さまざまな薬物について，大動脈瘤の拡大と破裂を抑制する効果に関しての研究が行われている。βブロッカーはその降圧作用と血圧のdP/dtを低下させる作用，さらに一部の薬剤が持つ細胞外マトリックスを補強する作用から大動脈瘤患者に対して処方されることの多い薬物であり，エビデンスレベルは低いものの日本のガイドラインでは胸部大動脈瘤における降圧薬の第一選択とされている[2]。

同様にエビデンスは豊富ではないが，動物実験で有効性を示したロサルタンやドキシサイクリン，ロキシスロマイシンなどの薬剤について現時点では期待がもたれており，米国などで臨床試験が行われている。

文　献

1) Committee for Scientific Affairs, Ueda Y, Fujii Y, Udagawa H: Thoracic and cardiovascular surgery in Japan during 2006: annual report by the Japanese Association for Thoracic Surgery. Gen Thorac Cardiovasc Surg, 2008, **56**: 365–388.
2) 循環器病の診断と治療に関するガイドライン(2004－2005年度合同研究班報告)：大動脈瘤・大動脈解離診療ガイドライン(2006

年改訂版). Circ J, 2006, **70**(Suppl. IV) : 1569–1646.

3) Svensson LG, Kouchoukos NT, Miller DC, et al: Expert consensus document on the treatment of descending thoracic aortic disease using endovascular stent-grafts. Ann Thorac Surg, 2008, **85**: S1–S41.

4) Takamoto S, Nawata K, Morota T: A simple modification of 'David-V' aortic root reimplantation. Eur J Cardiothorac Surg, 2006, **30**: 560–562.

5) David TE, Feindel CM, Webb GD, et al: Aortic valve preservation in patients with aortic root aneurysm: results of the reimplantation technique. Ann Thorac Surg, 2007, **83**: S732–S735.

A Case of Localized IgG4-Related Thoracic Periarteritis and Recurrent Nerve Palsy

Masao Takahashi, MD, Takashi Shimizu, MD, Tsukasa Inajima, MD, Yumiko Hosoya, MD, Norifumi Takeda, MD, Nobukazu Ishizaka, MD, Hiroshi Yamashita, MD, Yasunobu Hirata, MD and Ryozo Nagai, MD

Abstract: Periarteritis, including periaortitis, is a systemic disorder characterized by an excessive fibroinflammatory reaction that can result in the compromise of great vessels and periarterial/periaortic structures. Recent studies have suggested that IgG4-related inflammation may play a role in chronic periaortitis. These pathologic conditions might represent a systemic disorder with fibrotic reaction rather than local inflammation. In this report, the authors describe a case of a 31-year-old man with marked periaortic fibrous thickening localized to the aortic arch, which was histologically and serologically proven to be IgG4 related. Positron emission tomography showed increased ^{18}F-fluorodeoxyglucose uptake at this region. Histologic examination revealed infiltration of lymphoplasmacytes and marked fibrosis with numerous IgG4-positive plasma cells. The serum concentration of IgG4 was 263 mg/dL. The size of the periaortic mass and ^{18}F-fluorodeoxyglucose uptake at this region markedly decreased under corticosteroid therapy. This case suggests that IgG4-related periarteritis can also occur as a solitary focus in the cardiovascular system.

Key Indexing Terms: Periarteritis; Periaortitis; IgG4-related sclerosing disease. **[Am J Med Sci 2011;341(2):166–169.]**

Chronic periarteritis and periaortitis are a part of a spectrum of idiopathic diseases characterized by fibroinflammatory reaction surrounding the arteries and the aorta. Chronic periaortitis includes idiopathic retroperitoneal fibrosis and inflammatory abdominal aortic aneurysm, and it is considered as a systemic disorder caused by the extended involvement of the aorta and raised inflammatory markers.[1] On the other hand, IgG (immunoglobulin G) 4-related sclerosing disease is also known as a systemic disorder of protean manifestations that may involve the pancreas,[2] retroperitoneum,[3] bile duct[4] and salivary glands.[5] It has been recently suggested that IgG4-related sclerosing disease may be linked to chronic periarteritis and that these 2 disorders might overlap, at least in part.[1] We encountered a case of IgG4-related periarteritis at the thoracic aortic arch without evidence of other organ involvement.

CASE REPORT

A 31-year-old Japanese man was admitted to our hospital because of an episode of hoarseness with no previous history of any serious disease. He had not been prescribed any medication. He was a current smoker. On physical examination, blood pressure was 116/70 mm Hg, and other vital signs were within normal range. His left vocal cord was paralyzed because of recurrent laryngeal nerve paralysis. A chest radiograph showed abnormal protrusion of the aortic arch (Figure 1A), and computed tomography (CT) revealed a mass surrounding the aorta at its bifurcation to the subclavian artery (Figure 1B). ^{18}F-fluorodeoxyglucose (^{18}F-FDG) positron emission tomography (PET) showed increased tracer uptake at the aortic arch with no abnormal tracer uptake in other regions (Figure 1C). The following laboratory data were obtained: serum C-reactive protein, 0.62 mg/dL; erythrocyte sedimentation rate, 41 mm/hr; IgG, 1884 mg/dL; IgG4, 263 mg/dL; serum soluble interleukin-2 receptor, 458 U/mL; and absence of detectable antinuclear antibodies. IgG4 subtype accounted for 14.0% of the IgG fraction. CT and magnetic resonance imaging showed no abnormality in the lymph nodes, pancreas or retroperitoneum. Histologic analysis of the thoracoscopic biopsy specimen of the mass at the aortic arch demonstrated diffuse infiltration of lymphoplasmacytes and marked fibrosis, with no significantly atypical cells (Figures 2A and 2B).

Immunostaining for CD3 and CD20 showed that the lymphocytes were polyclonal and included mainly CD20-positive B cells and CD3-positive T cells. The number of CD20-positive B cells was larger than that of CD3-positive T cells (Figures 3A and 3B). In addition, immunostaining for IgG4 revealed many IgG4-positive plasma cells within the lesion (Figure 3C). On the basis of these findings, we made the pathologic diagnosis of IgG4-related periarteritis localized to the aortic arch. IgG4-positive disease frequently accompanies sclerosing pancreatitis. However, magnetic resonance cholangiopancreatography showed that in this patient, the pancreatic duct and bile duct were intact. No finding characteristic of sclerosing pancreatitis was observed. Consequently, we treated him with 40 mg of prednisolone daily for localized IgG4-related periarteritis. Eight weeks later, hoarseness was found to have gradually ameliorated, the chest radiograph and CT scan revealed improvement of the periaortic mass (Figures 4A and 4B), abnormal ^{18}F-FDG uptake of the aorta on PET scanning was reduced (Figure 4C) and all laboratory data were within normal range. We tapered the dose of prednisolone to 5 mg, and no signs of recurrence have been observed during the follow-up examinations (1 year).

DISCUSSION

IgG4-related sclerosing disease was first reported as sclerosing pancreatitis.[2] Since then, patients with histologically proven IgG4-positive plasma cell infiltration and/or markedly elevated serum IgG4 levels are being increasingly diagnosed. These abnormal findings lead to the development of IgG4-related diseases, which may affect different organs or tissues such as the bile duct, the salivary glands and the retroperito-

From the Department of Cardiovascular Medicine (MT, TS, TI, YH, NT, NI, HY, YH, RN), Graduate School of Medicine, The University of Tokyo, Hongo, Bunkyo-ku, Tokyo, Japan; and Division of Cardiology (NI), Department of Internal Medicine III, Osaka Medical College, Daigaku-machi, Takatsuki-shi, Osaka, Japan.

Submitted July 30, 2010; accepted in revised form September 9, 2010.

Correspondence: Masao Takahashi, MD, PhD, Department of Cardiovascular Medicine, Graduate School of Medicine, The University of Tokyo, Hongo 7-3-1, Bunkyo-ku, Tokyo 113-8655, Japan (E-mail: masaotakahashi-gi@umin.ac.jp).

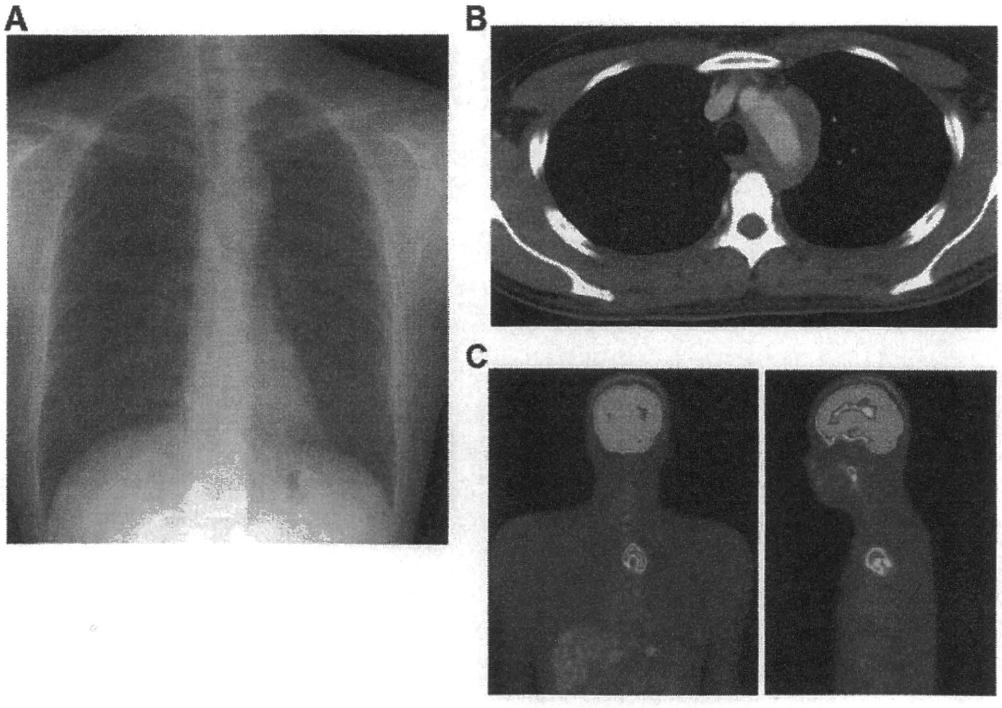

FIGURE 1. Before the corticosteroid therapy, the chest radiograph (A) showed an abnormal protrusion of the aortic arch, contrast medium-enhanced CT (B) of the chest revealed a periaortic mass in the mediastinum and ^{18}F-FDG-PET (C) showed increased tracer uptake at the aortic arch.

neum. Chronic periaortitis is characterized as a fibroinflammatory reaction usually affecting the abdominal aorta. Although the clinical spectrum of chronic periarteritis or periaortitis has not been well defined, retroperitoneal fibrosis and inflammatory abdominal aortic aneurysm are considered to belong to this entity.[1] Of note, there is an increasing body of evidence showing that chronic periaortitis is a feature of IgG4-related sclerosing diseases. For example, in retroperitoneal fibrosis, thickened fibrotic tissue is characterized by diffuse infiltration of IgG4-positive plasma cells.[6] Moreover, IgG4-related diseases can occur not only in tissues near the aorta but also in the wall of arteries including coronary arteries.[7] Therefore, periarteritis is an entity similar to periaortitis.

Although in most cases, the abdominal aorta and neighboring structures are affected, in few cases, only the thoracic aorta is involved.[8,9] One of the reported cases showed not only fibrosis of the thoracic aorta but also retroperitoneal fibrosis with raised IgG4 levels and involvement of other organs.[8] Another patient had an IgG4-related inflammatory aneurysm of the aortic arch whose maximum diameter was 55 mm.[9] In contrast to these 2 cases, no evidence of other organ involvement or of aneurysmal change of the aorta was found in our patient.

It has been suggested that chronic periarteritis and IgG4-related sclerosing disease might represent a systemic inflammatory disorder rather than local inflammatory disease, because each is characterized by constitutional symptoms and raised inflammatory markers with extended involvement of the aorta.[10] However, in our patient, the inflammatory reaction was restricted to the surrounding tissue of the aortic arch, and no abnormal involvement of other organs was detected. The mechanism of solitary and localized involvement in our patient remains to be identified. Some investigators have suggested that local inflammatory reaction to oxidized low-density lipoproteins and ceroids in the atherosclerotic plaques might cause periarteritis.[11] Our patient was a young man with few risk factors for atherosclerosis except for smoking. No atherosclerotic plaque was found in the biopsy specimen.

A recent study reported that T-helper 2 (T_H2) cells and regulatory immune reactions are upregulated in tissues affected by

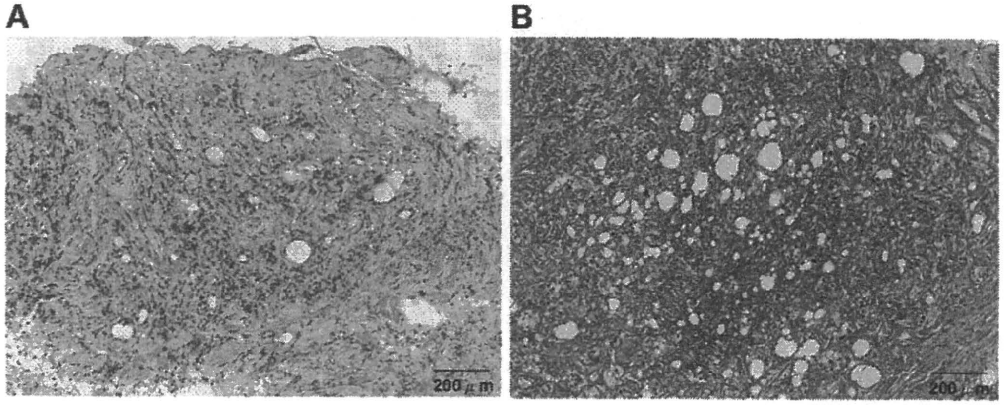

FIGURE 2. Histopathologic findings of the periaortic mass biopsy specimen. Hematoxylin and eosin staining showed lymphoplasmacytic infiltration intermixed with irregular fibrosis (A). Elastic van Gieson stain revealed marked fibrosis (B).

© 2011 Lippincott Williams & Wilkins
Copyright © by the Southern Society for Clinical Investigation. Unauthorized reproduction of this article is prohibited.

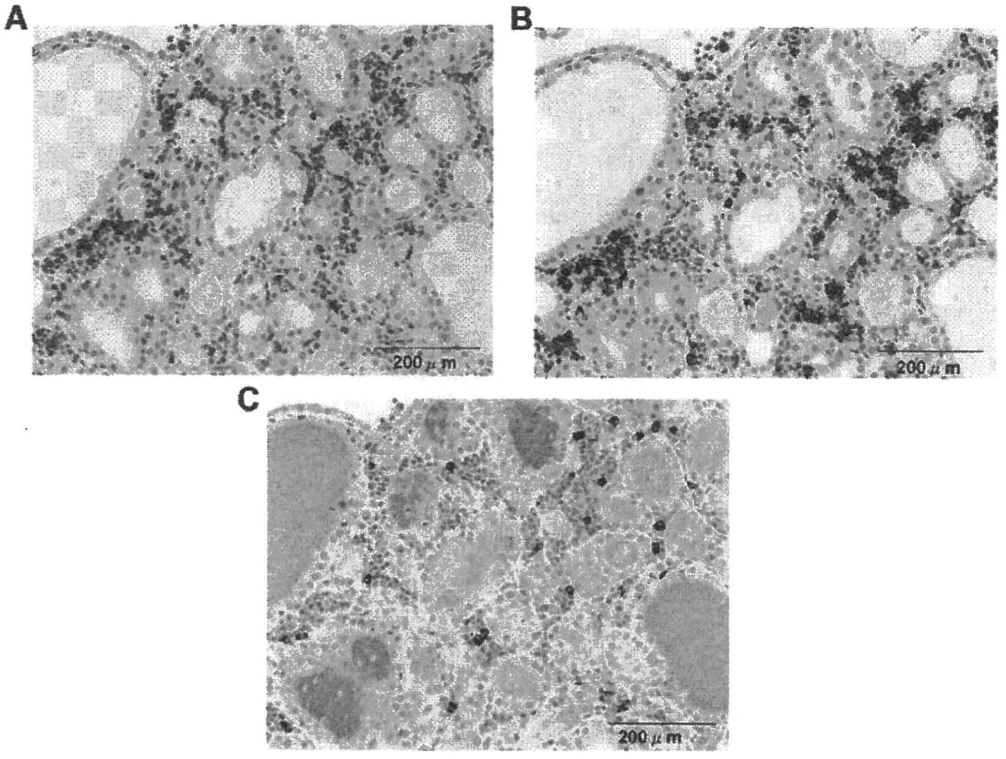

FIGURE 3. Immunostaining of the biopsy specimen for CD3 (A) and CD20 (B) showed that the infiltrate included mainly CD20-positive B cells and CD3-positive T cells. Immunostaining for IgG4 revealed many IgG4-positive plasma cells within the lesion (C).

IgG4-related sclerosing disease,[12] suggesting the involvement of T_H2 cell-mediated immune reaction in the pathogenesis of this disorder. Nevertheless, we did not evaluate the activity of T_H2-associated cytokines before corticosteroid therapy in our patient.

CT revealed a periaortic mass surrounding the aortic arch at a narrow region, and ^{18}F-FDG-PET disclosed remarkably localized tracer uptake. According to these findings, other diseases such as malignant lymphoma should be ruled out. Soluble interleukin-2 receptor level was found to be within normal range (458 U/mL), and serum IgG4 was elevated (263 mg/dL). Although these findings may not be characteristic of a malignant tumor,[6] pathologic examination was considered cru-

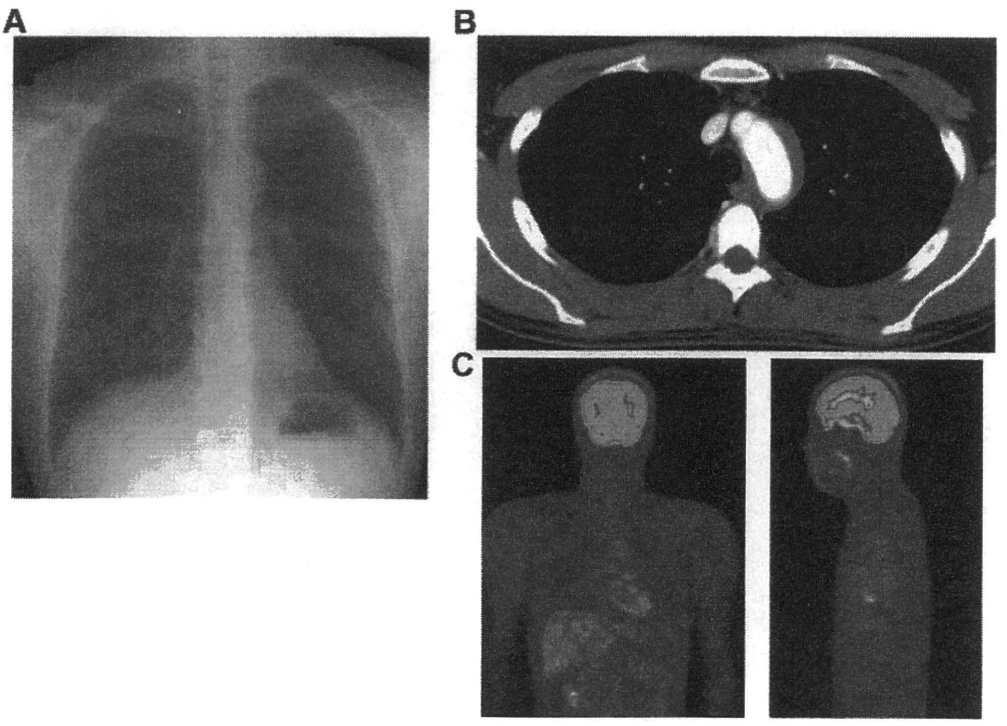

FIGURE 4. After the corticosteroid therapy, the chest radiograph (A) and CT scan (B) revealed a decrease in size of the periaortic mass. PET scanning (C) revealed no abnormal uptake of ^{18}F-FDG at the aortic arch.

Copyright © by the Southern Society for Clinical Investigation. Unauthorized reproduction of this article is prohibited.

cial for the differential diagnosis. Presence of the diffuse infiltration of the IgG4-positive lymphoplasmacytic cells without the evidence of atypicality was useful in distinguishing IgG4-related periarteritis from malignant lymphoma in our case. Serum IgG4 is useful for the diagnosis and evaluation of IgG4-related periarteritis. ^{18}F-FDG-PET is not specific for the diagnosis of IgG4-related periarteritis or chronic periaortitis,[13] but it is useful to assess the progression of the disease and search for other abnormalities in the whole body.

In conclusion, we have presented a case with IgG4-related periarteritis localized to the thoracic aorta. After the induction of corticosteroid therapy, the size of the fibrous mass surrounding the aortic arch decreased, the enhanced uptake of ^{18}F-FDG also decreased and recurrent nerve palsy disappeared. In this patient, accurate diagnosis led to suitable treatment.

REFERENCES

1. **Palmisano A, Vaglio A.** Chronic periaortitis: a fibro-inflammatory disorder. Best Pract Res Clin Rheumatol 2009;23:339–53.
2. **Hamano H, Kawa S, Horiuchi A, et al.** High serum IgG4 concentrations in patients with sclerosing pancreatitis. N Engl J Med 2001;344: 732–8.
3. **Hamano H, Kawa S, Ochi Y, et al.** Hydronephrosis associated with retroperitoneal fibrosis and sclerosing pancreatitis. Lancet 2002;359: 1403–4.
4. **Hamano H, Kawa S, Uehara T, et al.** Immunoglobulin G4-related lymphoplasmacytic sclerosing cholangitis that mimics infiltrating hilar cholangiocarcinoma: part of a spectrum of autoimmune pancreatitis? Gastrointest Endosc 2005;62:152–7.
5. **Kitagawa S, Zen Y, Harada K, et al.** Abundant IgG4-positive plasma cell infiltration characterizes chronic sclerosing sialadenitis (Kuttner's tumor). Am J Surg Pathol 2005;29:783–91.
6. **Zen Y, Onodera M, Inoue D, et al.** Retroperitoneal fibrosis: a clinicopathologic study with respect to immunoglobulin G4. Am J Surg Pathol 2009;33:1833–9.
7. **Matsumoto Y, Kasashima S, Kawashima A, et al.** A case of multiple immunoglobulin G4-related periarteritis: a tumorous lesion of the coronary artery and abdominal aortic aneurysm. Hum Pathol 2008;39: 975–80.
8. **Zen Y, Sawazaki A, Miyayama S, et al.** A case of retroperitoneal and mediastinal fibrosis exhibiting elevated levels of IgG4 in the absence of sclerosing pancreatitis (autoimmune pancreatitis). Hum Pathol 2006; 37:239–43.
9. **Ishida M, Hotta M, Kushima R, et al.** IgG4-related inflammatory aneurysm of the aortic arch. Pathol Int 2009;59:269–73.
10. **Vaglio A, Corradi D, Manenti L, et al.** Evidence of autoimmunity in chronic periaortitis: a prospective study. Am J Med 2003;114:454–62.
11. **Vaglio A, Salvarani C, Buzio C.** Retroperitoneal fibrosis. Lancet 2006;367:241–51.
12. **Zen Y, Fujii T, Harada K, et al.** Th2 and regulatory immune reactions are increased in immunoglobin G4-related sclerosing pancreatitis and cholangitis. Hepatology 2007;45:1538–46.
13. **Pipitone N, Ghinoi A, Versari A, et al.** Images in cardiovascular medicine. Chronic periaortitis. Circulation 2008;118:1214–6.

RETRACTION

Respiratory Stress Response: A Novel Diagnostic Method for Detection of Significant Coronary Artery Disease From Finger Pulse Wave Analysis During Brief Respiratory Exercise: RETRACTION

The authors have informed us that the above article by Dr. Shiyovich et al published in *The American Journal of the Medical Sciences* contains results that were significantly biased. The authors continued investigating the above novel diagnostic test in additional studies in the target population – ambulatory patients referred to evaluate the presence of significant coronary artery disease and found much lower diagnostic efficacy. In cooperation with the developing company (SPIROCOR) the authors meticulously reanalyzed the above study results and found that the results of the new test were matched incorrectly with the gold standard (QCA) in a significant amount of cases, hence the results reported in the published article were significantly biased and not reliable. This incorrect matching is the subject of an ongoing investigation. Retrospectively, the authors believe it was nearly impossible to notice this incorrect matching at the time. Following these findings SPIROCOR is shutting down all clinical studies and activities. Importantly, the new test has not been implemented into clinical use anywhere in the world.

We are therefore retracting the paper by Dr. Shiyovich et al published in *The American Journal of the Medical Sciences.*

REFERENCE

Shiyovich A, Jafari J, Blaer Y, et al. Respiratory Stress Response: A Novel Diagnostic Method for Detection of Significant Coronary Artery Disease From Finger Pulse Wave Analysis During Brief Respiratory Exercise. Am J Med Sci 2010;339:440–7.

© 2011 Lippincott Williams & Wilkins
Copyright © by the Southern Society for Clinical Investigation. Unauthorized reproduction of this article is prohibited.

症例

冠動脈造影時の造影剤によるアナフィラキシーショックと薬剤抵抗性冠攣縮の1例

A case of anaphylactic shock and subsequent drug-refractory coronary spasm induced by contrast media during coronary angiography

田崎龍之介　谷川　淳　村井基修　藤阪智弘　柚木孝仁　武田義弘
新名荘史　岡部太一　中小路隆裕　星賀正明　石原　正　花房俊昭

大阪医科大学第一内科学教室

《Abstract》

症例は65歳，女性．2007年4月，労作性狭心症に対し左前下行枝に薬剤溶出性ステント(Cypher®)を留置した．同年11月，同部位に遅発性ステント血栓症を生じ不安定狭心症となり，バルーン拡張術を施行した．2008年3月，フォローアップ冠動脈造影施行．造影剤は使用歴のあるイオメプロール(イオメロン®)を使用した．右冠動脈に約7mLの造影剤を投与したところ，直後に頸部掻痒感を訴え，血圧低下をきたしショック状態となった．ノルエピネフリン投与で血圧は確保されたものの，右冠動脈に閉塞性冠攣縮を生じた．硝酸イソソルビドの冠動脈内投与を行ったが，攣縮解除にはいたらず，ニコランジルの冠動脈投与を繰り返し，改善した．改善後の冠動脈造影，血管内超音波では有意な器質的狭窄や血管解離はなく，造影剤アレルギーによるアナフィラキシーショックから薬剤抵抗性冠攣縮をきたしたものと考えられた．今回稀ではあるが，造影剤による難治性冠攣縮を経験したので報告する．

Ryunosuke Tazaki, Jun Tanigawa, Motonobu Murai, Tomohiro Fujisaka, Takahito Yuki, Yoshihiro Takeda, Takafumi Shimmyo, Taichi Okabe, Takahiro Nakakouji, Masaaki Hoshiga, Tadashi Ishihara, Toshiaki Hanafusa

First Department of Internal Medicine, Osaka Medical College

Key words
- 造影剤アレルギー
- 急性冠症候群
- ニコランジル
- IVUS

(2009.4.8 原稿受領；2009.6.15 採用)

(日本循環器学会第106回近畿地方会　推薦演題)

はじめに

現在日常臨床において汎用されている非イオン性造影剤は，以前のイオン性造影剤に比べ安全性が向上した．冠動脈造影において，イオン性造影剤では22%に早期反応を，45%に心電図変化を認めたが，非イオン性造影剤ではそれぞれ8.8%，12.6%と大幅に改善された[1]．しかし頻度は低くなったものの，ときに致命的なアナフィラキシー反応を引き起こすことがある．冠動脈造影の合併症の1つである冠攣縮は，造影剤の副作用というよりもむしろカテーテル操作特有の合併症として考えられており，その頻度は0.26～3%と報告されている[2]．ほとんどの冠攣縮は亜硝酸薬の冠動脈内投与で速やかに解除されるが，稀に治療抵抗性で遷延する症例を経験する．今回われわれは，造影剤によるアナフィラキシーショックから引き続いた難治性冠攣縮をきたし，硝酸イソソルビド(isosorbide dinitrate；ISDN)では解除できず，

Presented by Medical*Online

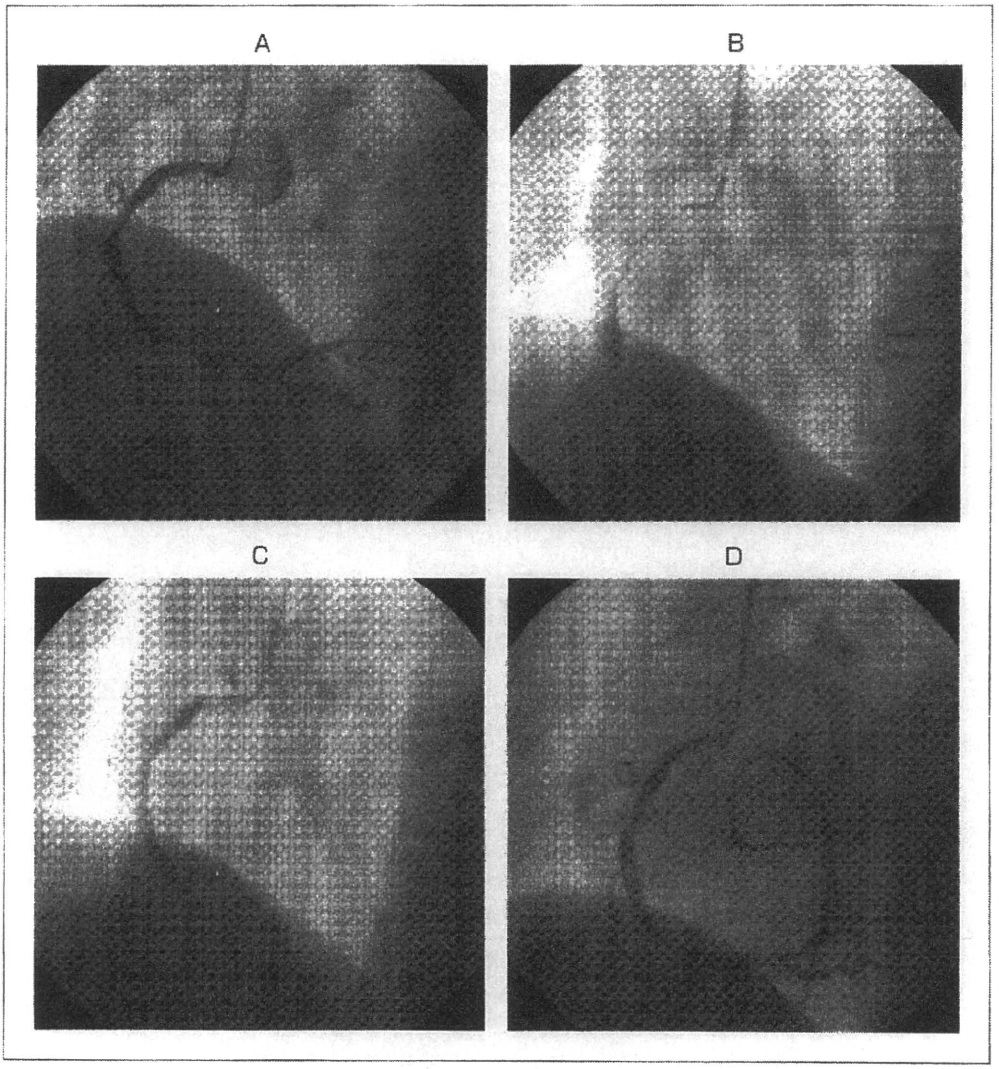

図 1
右冠動脈造影
A：初回テストショット造影
B：ST上昇時
C：ISDN冠動脈投与後
D：ニコランジル冠動脈投与後

ニコランジルの冠動脈内頻回投与により解除し得た症例を経験したので報告する.

症例

患者：65歳，女性.

主訴：なし(冠動脈インターベンション後追跡造影).

既往歴：52，54歳；脳梗塞，61歳；ナルコレプシー.

内服歴：アスピリン100mg，クロピドグレル75mg，アテノロール25mg，硝酸イソソルビド40mg，バルサルタン160mg，エゼチミブ10mg.

現病歴：労作性狭心症にて，2006年12月，左前下行枝(left anterior descending artery；LAD)近位部にバルーン拡張を施行した．翌年 4 月同部位の再狭窄に対して薬剤溶出性ステント(drug eluting stent；DES)を留置した．2007年11月，同部位のステント血栓症で不安定狭心症となり，バルーン拡張術を行った．今回，経皮的冠動脈インターベンション(percutaneous coronary intervention；PCI) 3 カ月後の追跡造影目的にて2008年 3 月に入院となった.

入院時現症：血圧；140/88mmHg，脈拍；64/分・整，心雑音；聴取せず，呼吸音；清明，そのほか腹部所見に異常なし.

入院時検査：安静時心電図は心拍数57/分の正常洞

Presented by Medical*Online

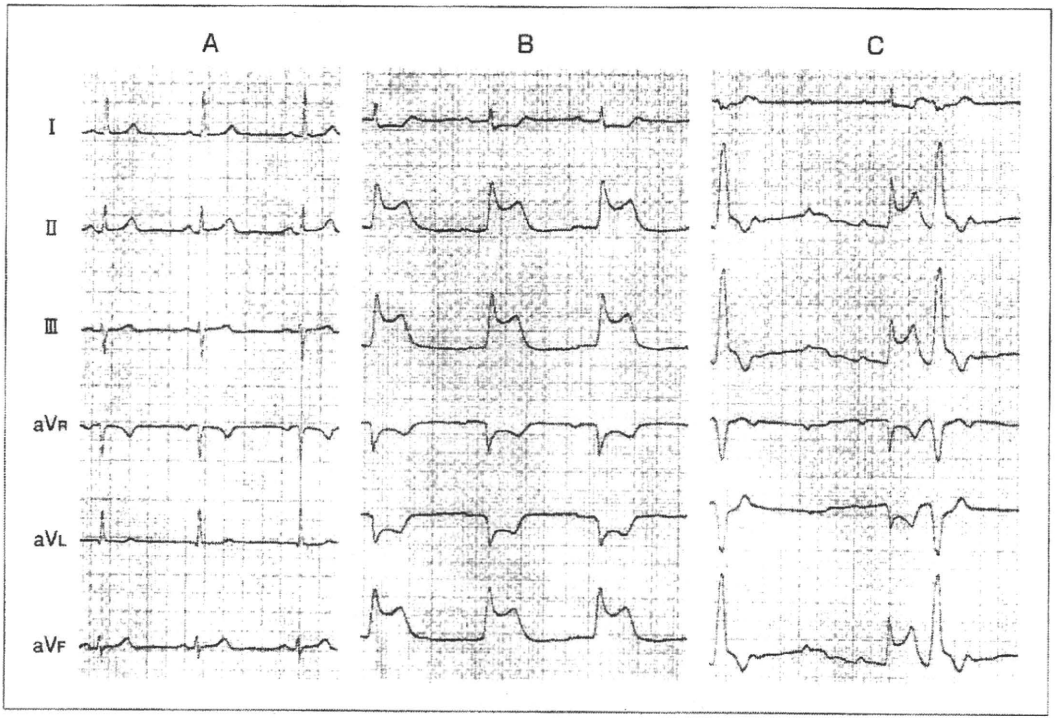

図2
心電図経過
A：冠動脈造影開始前
B：造影剤投与直後；下壁誘導でのST上昇
C：ISDN冠動脈投与後；完全房室ブロック

調律でST偏位なし．胸部X線では心胸郭比58%と軽度心拡大を認めるが肺うっ血なし．心臓超音波で心室中隔から心尖部にかけて壁運動の低下あり．血液生化学検査は明らかな異常なし．トレッドミル負荷心電図は陰性であった．

入院後経過：冠動脈造影は右橈骨動脈アプローチにて施行した．まず右冠動脈(right coronary artery；RCA)に0.05%硝酸イソソルビド(ニトロール®) 1 mgを投与し，引き続き造影剤イオメプロール(イオメロン350®)でテスト造影をしたところ，直後に頸部掻痒感が出現し，収縮期血圧50mmHg台に低下した．テスト造影の所見(**図1A**)は，RCA#1入口部とRCA#3に中等度狭窄を認めるものの，3カ月前のPCI直後の造影検査所見と著変は認めなかった．急速補液とともに，ノルエピネフリン(ノルアドレナリン®)の静脈投与を開始した．血圧は上昇したが，心電図上II，III，aVF誘導にてST上昇を認めた(**図2B**)ため再度造影を行ったところ，RCA#1は99%狭窄で造影遅延を伴っており(**図1B**)，冠攣縮と判断し硝酸イソソルビド1 mgを冠動脈投与した．いったんはRCA#3まで血流改善を認めた(**図1C**)が，ST上昇は遷延し完全房室ブロックとなった(**図2C**)．硫酸アトロピン0.5mgを静脈投与し，ISDNを合計4 mg追加冠動脈投与したが血流は改善せず，完全房室ブロックは持続した．そのため右大腿静脈アプローチで経皮的一時ペーシングを開始し，バルーンによる機械的再灌流に備えて造影カテーテルを7Frガイドカテーテルに変更した．その際にもカテーテル先端の刺激にて容易にスパスムを繰り返したためニコランジル(シグマート®)を合計4 mg冠動脈投与し，経静脈的にも4 mg/時で開始した．またノルエピネフリンによる冠攣縮の可能性も考慮し，ノルエピネフリンから塩酸ドパミン(カコージン®)に変更した．一方造影剤アレルギーの関与も考え，リン酸ヒドロコルチゾンナトリウム500mg(水溶性ハイドロコートン®)を静脈投与した．入口部の高度狭窄が持続した(**図1D**)ため，カテーテルによる血管損傷も含め器質的狭窄の確認のため血管内超音波(intravascular ultrasound；IVUS)を行った．IVUSカテーテル挿入時にも冠攣縮を繰り返し，ニコランジルの頻回投与を要した．IVUSで

Presented by Medical*Online

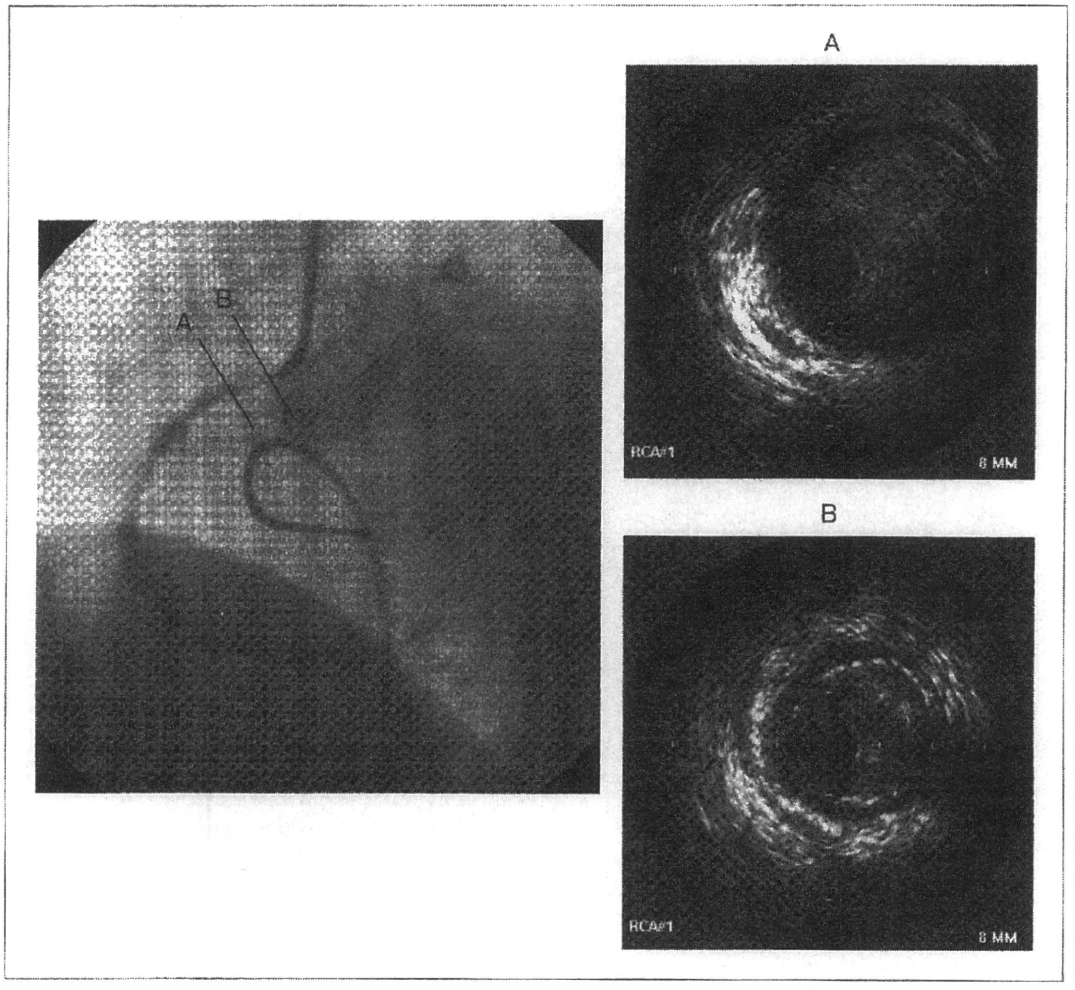

図 3
右冠動脈入口部血管内超音波所見
入口部BはAに比較し内弾性板の狭小化があり入口部攣縮が残存することを示唆するが，いずれも有意な器質的狭窄ではない．

は，軽度のプラークを認めるものの解離や有意な器質的狭窄はなく，入口部の攣縮が確認された(**図 3**)．

最終造影では入口部に軽度攣縮は残存するが，末梢までTIMI 3の血流が得られた．さらなるカテーテル刺激による左主幹部攣縮を危惧し，左冠動脈造影は行わなかった．カテーテル抜去後，心電図は正常に復した．帰室後も胸部症状はなく，心筋逸脱酵素の上昇は認めなかった．後に施行したイオメプロール(イオメロン350®)の薬剤リンパ球刺激試験は陰性であった．内服のアテノロールは中止し，ニコランジル(シグマート® 15mg/日)，ニフェジピン(アダラートL® 40mg/日)を追加した．退院後胸部症状の出現なく経過している．その後さらなる病歴聴取より，幼少時イソジンにより口唇の発赤・腫脹を認めていたことが判明し，ヨードアレルギーの既往が示唆された．

考察

今回，造影剤アレルギーによるアナフィラキシーショックを起こし，さらに薬剤抵抗性冠攣縮に進展した症例を経験した．現在使用される非イオン性造影剤は以前のイオン性造影剤に比べ安全性に優れており，重篤な副作用が少なく，忍容性が高いことが報告されている[3]．Kunadianらの報告では，イオメプロールを用い1,024症例を対象に待機的診断カテーテル検査を行い，一過性の血圧低下を20人(2.1%)に，一過性のST上昇を1人(0.1%)に，心室頻拍を1人(0.4%)に，心停止を1人(0.1%)に認め，比較対象

としたイオパミドールと同等の副作用発生頻度であったと報告している[4]．またBishopらは，非イオン性造影剤を使用し，冠攣縮性狭心症の既往がない4例に冠攣縮を認め，頻度は640人中4人(0.6%)であったと報告しているが，造影剤によるアナフィラキシーに伴う冠攣縮の報告は少ない[5]．一方，Sinkiewiczらは，蜂刺症などによるアナフィラキシー反応に伴う急性冠症候群(Kounis syndrome)には2つの型があり，Ⅰ型は動脈硬化病変がなく，ヒスタミンなどによる内皮障害から冠攣縮にいたるもの，Ⅱ型は動脈硬化病変が存在し，血管壁収縮から粥腫破綻を生じるものと報告している[6]．山田らは，冠動脈造影時の造影剤によるアナフィラキシーショックから胸痛・ST上昇をきたしたが，血管造影上，表在性冠動脈に狭窄・閉塞所見を認めない症例を経験し，ニコランジルの冠動脈投与によりTIMI 2からTIMI 3への改善を認めたことから，microvascular spasmの可能性について報告している[7]．

本症例においてアナフィラキシー以外の原因で冠攣縮にいたった原因として，β遮断薬であるアテノロールの内服，冠攣縮性狭心症の既往，ノルエピネフリンの関与，あるいはカテーテルの物理的刺激による誘発が考えられる．しかし本例はアテノロール25mgを約3年間にわたって内服していたが，安静時狭心症を疑う症状はなかった．一方，血圧低下の際，昇圧目的で使用したノルエピネフリンが冠トーヌスを亢進させ冠攣縮が誘発された可能性は否定できない．また通常遭遇するカテーテル先端刺激による冠攣縮の可能性について，Friedmanらは，カテーテル誘発冠攣縮は右冠動脈で起こりやすく，カテーテル先端からなめらかで同心性，長さは2mm未満であるのが特徴で，それ以外の冠攣縮ではカテーテル先端から1～4cm離れた部位で生じ，通常不規則，偏心性であることが多いと報告しており[8]，本症例でも後者と共通点が多い．

冠攣縮の対処法として，通常は亜硝酸薬，Ca拮抗薬が選択され，治療抵抗性冠攣縮においてはKチャネル開口薬であるニコランジルの有効性が報告されている．ニコランジルは冠拡張作用に比し血圧低下作用が緩やかであり，冠動脈拡張作用も強い[9]．Noguchiらは治療抵抗性の2症例にニコランジル1mgの冠動脈投与を行い，改善したと報告している[10]．またHayashiらは，冠攣縮によるショック症例においてニコランジル2mgの冠動脈投与が有効であったと報告している[11]．アナフィラキシー反応については，アメリカ心臓協会心肺蘇生ガイドライン2005によると，低血圧や呼吸困難など明らかに全身状態が悪化する症例はエピネフリン(0.3～0.5mg)の筋肉内投与が望ましく，またβ遮断薬内服中であればアナフィラキシーの重症度がかえって増悪することがあるためグルカゴン(1～2mg筋肉内投与)が有効とされている[12]．本例はエピネフリン，グルカゴンは使用せずリン酸ヒドロコルチゾンナトリウムを投与したが，その効果発現には4～6時間を要するとされ，検査中の冠攣縮改善に影響したとは考えにくく，ニコランジルの冠動脈投与が奏功したものと考える．本例ではカテーテル先端の損傷に伴う冠動脈解離を疑い，IVUSを行った．その結果，冠動脈解離は認めず，軽度の内膜肥厚と内弾性板の狭小化を認め，冠攣縮と判断した．血管造影上は正常冠動脈であっても，IVUSでは微小な動脈硬化性病変を有し，それが冠攣縮と関連すると報告されている[13]．Saitoらは45人を対象にエルゴノビン，アセチルコリン誘発試験を行い，有意な冠攣縮が23人に出現し，全例に動脈硬化初期病変である内膜肥厚を認めたと報告した[14]．血管平滑筋刺激の局所反応の原因として，中膜，内皮細胞，神経伝達因子に加え，内膜肥厚の関与が示唆されている．

結語

非イオン性造影剤は以前の造影剤に比べ有害事象の発現頻度は低く，安全に使用できるようになった．しかし本例のように，ヨード造影剤に対するアナフィラキシー反応の1つとして重篤な冠攣縮をきたす可能性があり，念頭に置くべき合併症と思われ報告した．

Presented by Medical*Online

文 献

1) Sutton AG, Finn P, Grech ED, et al : Early and late reactions after the use of iopamidol 340, ioxaglate 320, and iodixanol 320 in cardiac catheterization. *Am Heart J* 2001 ; **141** : 677-683
2) Ilia R, Cafri C, Jafari J, et al : Prolonged catheter-induced coronary artery spasm mimicking fixed stenosis. *Cathet Cardiovasc Diagn* 1997 ; **41** : 170-173
3) Katayama H, Yamaguchi K, Kozuka T, et al : Adverse reactions to ionic and nonionic contrast media. A report from the Japanese Committee on the Safety of Contrast Media. *Radiology* 1990 : **175** : 621-628
4) Vijayalakshmi K, Kunadian B, Wright RA, et al : A prospective randomised controlled trial to determine the early and late reactions after the use of iopamidol 340 (Niopam) and iomeprol 350 (Iomeron) in cardiac catheterisation. *Eur J Radiol* 2007 ; **61** : 342-350
5) Bishop N, Rees MR : Idiosyncratic reaction to intracoronary injection of non-ionic contrast media. *Clin Radiol* 1988 ; **39** : 396-397
6) Sinkiewicz W, Sobański P, Bartuzi Z : Allergic myocardial infarction. *Cardiol J* 2008 ; **15** : 220-225
7) 山田健志，北嶋宏樹，宮井伸幸，ほか：冠動脈造影中にアナフィラキシーショックとST上昇を認めた1例．心臓 2008 ; **40** : 533-538
8) Friedman AC, Spindola-Franco H, Nivatpumin T : Coronary spasm : Prinzmetal's variant angina vs. catheter-induced spasm ; refractory spasm vs. fixed stenosis. *AJR Am J Roentgenol* 1979 ; **132** : 897-904
9) Yanagisawa T, Teshigawara T, Taira N : Cytoplasmic calcium and the relaxation of canine coronary arterial smooth muscle produced by cromakalim, pinacidil and nicorandil. *Br J Pharmacol* 1990 ; **101** : 157-165
10) Noguchi T, Nonogi H, Yasuda S, et al : Refractory coronary spasm relieved by intracoronary administration of nicorandil. *Jpn Circ J* 2000 ; **64** : 396-398
11) Hayashi T, Ichikawa M, Iwata A, et al : Intracoronary nicorandil relieves multiple coronary vasospasm with hemodynamic collapse. *Circ J* 2008 ; **72** : 327-330
12) 2005 American Heart Association : Anaphylaxis. *Circulation* 2005 ; **112** : Ⅳ143-Ⅳ145
13) Yamagishi M, Miyatake K, Tamai J, et al : Intravascular ultrasound detection of atherosclerosis at the site of focal vasospasm in angiographically normal or minimally narrowed coronary segments. *J Am Coll Cardiol* 1994 ; **23** : 352-357
14) Saito S, Yamagishi M, Takayama T, et al : Plaque morphology at coronary sites with focal spasm in variant angina : study using intravascular ultrasound. *Circ J* 2003 ; **67** : 1041-1045

Presented by Medical*Online

ELSEVIER

International Journal of Cardiology 141 (2010) 151–156

International Journal of
Cardiology

www.elsevier.com/locate/ijcard

Quantitative analysis of intracoronary optical coherence tomography measurements of stent strut apposition and tissue coverage

Peter Barlis *, Konstantinos Dimopoulos, Jun Tanigawa, Ewa Dzielicka, Giuseppe Ferrante, Francesca Del Furia, Carlo Di Mario

Department of Cardiology, Royal Brompton Hospital, London, United Kingdom

Received 29 July 2008; accepted 27 November 2008
Available online 19 January 2009

Abstract

Background: The introduction of optical coherence tomography (OCT) as an intracoronary imaging modality has allowed accurate assessment of strut apposition and neointimal tissue coverage. This study set out to assess the inter and intraobserver variability of measurements of acute stent apposition and strut tissue coverage using OCT.

Methods: Thirty patients were studied (14 immediately after stent implantation and 16 during follow-up angiography [mean of 4.7± 2.8 months]) using OCT (LightLab, Westford, Massachusetts, US). Data analysis was performed by 2 experienced observers. Struts were classified as "embedded", "protruding" or "malapposed" to the vessel well and recorded as percentage of total struts. Intimal coverage at follow-up was measured as the thickness of tissue covering each strut expressed in μm. Intra and interobserver variability was assessed by Bland-Altman plots and by calculation of the intraclass correlation coefficient (ICC).

Results: An average of 3967 struts was examined by each observer and, overall, 53.7% of struts was embedded, 36.4% protruding and 9.9% malapposed. Low intraobserver variability for all measures of strut apposition was found, with repeatability coefficients that ranged between 5.1% and 9.3% and ICC exceeding 95% in all cases. Interobserver variability was also low (repeatability coefficients 6.6–10.8 and ICC>91.3%). Mean intimal thickness in the follow-up group was 172.5 μm. Bland-Altman plots demonstrated a low intraobserver and interobserver variability for intimal thickness, with repeatability coefficients 26.7 μm and 24.1 μm, respectively and ICC exceeding 98.6% for both.

Conclusions: Low intra and interobserver variability can be expected when analyzing OCT data for stent apposition and tissue coverage. This supports the validity of OCT as a clinical and research tool in the setting of intracoronary stent imaging.
© 2008 Published by Elsevier Ireland Ltd.

Keywords: Optical coherence tomography; Strut apposition; Tissue coverage; Reproducibility

Optical coherence tomography (OCT) is rapidly achieving widespread diffusion in catheterisation laboratories worldwide. Its advantage over intravascular ultrasound (IVUS) is its superior resolution (15 μm) and fewer artifacts. The current technology permits image acquisition using a 1310 nm near-infrared light source that detects backscattering of light from superficial microstructures within the coronary wall. OCT has been used as an intracoronary imaging tool for the assessment of stent apposition, neointimal tissue coverage and plaque characterization [1–10]. To date, there is only one commercially available OCT system which uses a proprietary software for offline analysis of acquired images. We sought to assess the inter- and intra-observer variability of the current OCT system for stent strut apposition immediately following stent deployment and for tissue coverage at follow-up.

* Corresponding author. Department of Cardiology, Royal Brompton Hospital, Sydney Street, London SW3 6NP, United Kingdom. Tel.: +44 20 7352 8616; fax: +61 3 9470 8311.
E-mail address: peter.barlis@gmail.com (P. Barlis).

0167-5273/$ - see front matter © 2008 Published by Elsevier Ireland Ltd.
doi:10.1016/j.ijcard.2008.11.204

1. Methods

A total of 30 patients were prospectively included in this study. OCT was performed immediately after stent deployment in 14 patients and on follow-up angiography in a separate group of 16 patients, using the LightLab system (Westford, Massachusetts, US). Blood clearance was achieved using a proximal occlusion balloon (Helios, Goodman, Japan) with intra-coronary flush of lactated Ringer's solution through the end-hole of the balloon catheter (flow rate 0.6–0.9 ml/s) during simultaneous image acquisition at 1.0 mm/s using the dedicated ImageWire (LightLab Imaging, Westford, Massachusetts, US) at 15.6 frames/second.

1.1. OCT data analysis

Offline OCT images were analyzed by 2 experienced observers. For intraobserver variability, measurements were repeated 3 months after the initial assessment by the same observer, who was blinded to the previous results. For inter-observer variability, measurements were carried out independently by the two observers, blinded to each other's analysis.

1.2. Acute stent strut apposition

Analysis of contiguous cross-sections within the stented segment was performed at 1 mm intervals. In each selected cross section, the distance between the endoluminal border of the strut and the intima was measured. As OCT can only image the endoluminal strut border, distances were adjusted based on the thickness of the strut, including the polymer, for each of the stent types used [9]. Struts were classified as "embedded" when buried into the vessel wall, "protruding" when in contact with the vessel wall but protruding into the lumen and "malapposed" when no contact between the intima and the strut was detected (Fig. 1).

1.3. Strut tissue coverage

Tissue coverage was assessed by OCT at a minimum of 3 months post-implantation of different stents types. The thickness of the tissue overlying each stent strut was measured.

1.4. Statistical analysis

Statistical analyses and generation of plots were performed using R version 2.6.1 (The R Foundation for Statistical Computing, Vienna, Austria). To assess intra and inter-observer agreement, Bland-Altman plots were produced and mean difference and 95% limits of agreement with 95% confidence intervals were calculated. The repeatability coefficient (within which 95% of all differences are included) was calculated as twice the standard deviation of the differences between measurements on the same segment, as described by Bland and Altman [11]. Intra-class correlation

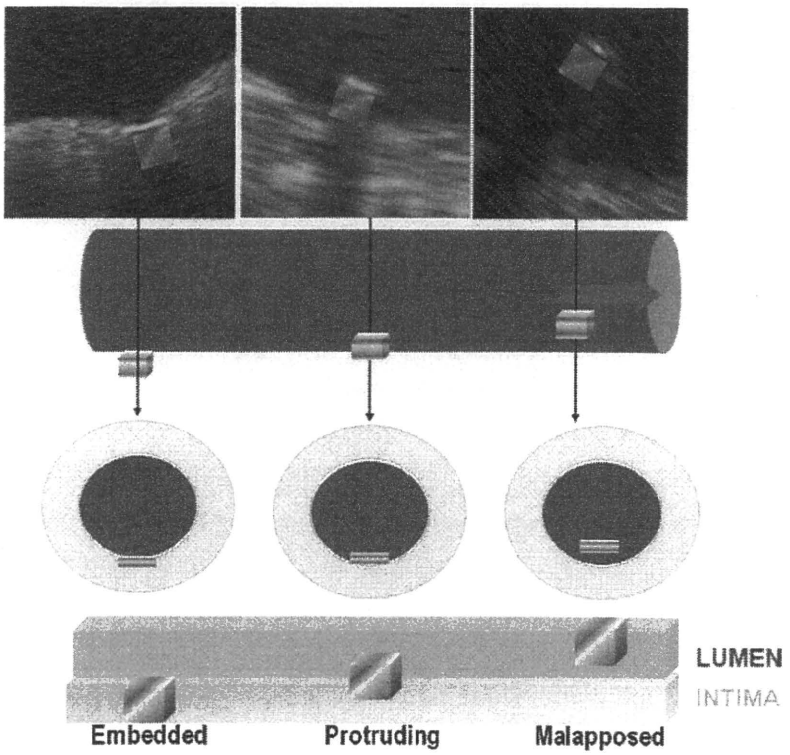

Fig. 1. Optical coherence tomography classification of stent apposition into embedded, protruding or malapposed.

Table 1
Baseline clinical, lesion and procedural characteristics.

	Assessment of acute apposition ($n=14$)	Assessment of intimal coverage ($n=16$)
Age (years)	62±11	60±7
Men	11 (78.6%)	15 (93.7%)
Hypertension	6 (42.9%)	8 (50%)
Diabetes Mellitus	1 (7.1%)	5 (31.2%)
Hypercholesterolemia*	12 (85.7%)	10 (62.5%)
Current smoker	4 (28.6%)	3 (18.7%)
Prior myocardial infarction	5 (35.7%)	7 (43.7%)
Prior coronary artery bypass grafting	0 (0%)	3 (18.7%)
Prior percutaneous coronary intervention	3 (21.4%)	16 (100%)
1-vessel disease	8 (57.1%)	6 (37.5%)
2-vessel disease	4 (28.6%)	6 (37.5%)
3-vessel disease	2 (14.3%)	4 (25.0%)
Clinical presentation		
Stable Angina Pectoris	8 (57.1%)	10 (62.5%)
Unstable Angina Pectoris	6 (42.9%)	6 (37.5%)
Time to optical coherence tomography (months)	–	4.7±2.8
Artery treated and imaged		
Left anterior descending	7 (50%)	8 (50.0%)
Left circumflex	3 (21.4%)	3 (18.8%)
Right	4 (28.6%)	5 (31.2%)
Number of stents/patient	1.8±0.9	1.6±0.6
Stent type		
Cypher stent	8 (57.1%)	6 (37.5%)
Taxus stent	4 (28.6%)	3 (18.8%)
Endeavour stent	1 (7.1%)	2 (12.5%)
Costar stent	2 (14.2%)	1 (6.2%)
Yukon	0 (0%)	4 (25.0%)

* Total cholesterol ≥5.0 mmol/L or treatment with a lipid-lowering drug.

coefficients (ICC) with 95% confidence intervals were also calculated as an additional measure of intra and inter-examiner reliability.

2. Results

2.1. Acute stent strut apposition

Clinical and angiographic and procedural characteristics of the 14 patients having OCT immediately following stent implantation are shown in Table 1. The target vessel was the left anterior descending artery (LAD) in 50%, left circumflex artery (LCx) in 21.4% and the right coronary artery (RCA) in 28.6%. OCT was performed uneventfully in all cases.

A mean of 3930 struts were examined by observer 1 and 4042 by observer 2. The average percent embedded, protruding and malapposed struts for observer 1 was 52.1%, 38.2% and 9.7%, respectively, and for observer 2, 55.3%, 34.6%, and 10.1%, respectively.

The Bland-Altman plots showed low intra-observer variability for all measures of strut apposition, with repeatability coefficients that ranged between 5.1% and 9.3% (Fig. 2, Table 2). The intraclass correlation coefficient, exceeding 95% in all cases, confirmed the high intra-observer repeatability of the OCT measurements. No consistent bias was observed (mean absolute difference between observations ranging between 0.0–1.8%).

Good agreement was also found between observers for measures of strut apposition, with narrow limits of agreement on the Bland-Altman plots. Repeatability coefficients ranged between 6.6–10.8%, with intraclass correlation coefficients exceeding 91%. No consistent bias was observed (mean absolute difference between observations ranged between 1.2–3.5%).

2.2. Strut tissue coverage

Sixteen patients underwent OCT evaluation of late stent strut tissue coverage at a mean follow-up 4.7±2.8 months from stent implantation. Clinical, angiographic and procedural characteristics of this population are also depicted in Table 1. Mean intimal thickness for observers 1 and 2 was 169.6 μm and 175.5 μm, respectively. The Bland-Altman plots demonstrated a low intraobserver variability for intimal thickness, with no bias (Fig. 3). The repeatability coefficient was 26.7 μm, with a high ICC (98.6%). A high degree of agreement between different observers was also found. Limits of agreement were narrow and the repeatability coefficient was 24.1 μm. ICC was very high (99.6%).

3. Discussion

This is the first systematic study to evaluate inter and intra-observer variability for both acute stent apposition and late tissue stent strut coverage using OCT. With its high resolution, OCT permits a detailed assessment of coronary structures while giving unique insights into tissue responses following stent implantation. Our study shows that OCT analysis gives highly reproducible data for both the assessment of acute stent strut apposition and late strut tissue coverage.

3.1. Stent strut apposition

Until recently, IVUS has been the gold standard for the assessment of acute and late stent strut apposition. Many studies have examined the implications of incomplete stent apposition with some showing no relation to adverse events [12,13] while others finding a link with in-stent restenosis and stent thrombosis [14–16]. Such inconsistencies are likely explained by the known limitations of IVUS, namely its low resolution (100 μm) and the presence of artifacts. OCT uses near infra-red light with 10 times higher resolution than IVUS. This unique imaging modality gives precise quantification of stent struts and their relation to the vessel wall without the artifacts associated with echo.

The infra-red light used by OCT is, however, unable to penetrate metal, thus producing dorsal shadowing behind the endoluminal aspect of the stent struts. As a result, when evaluating strut apposition, the additional thickness of the

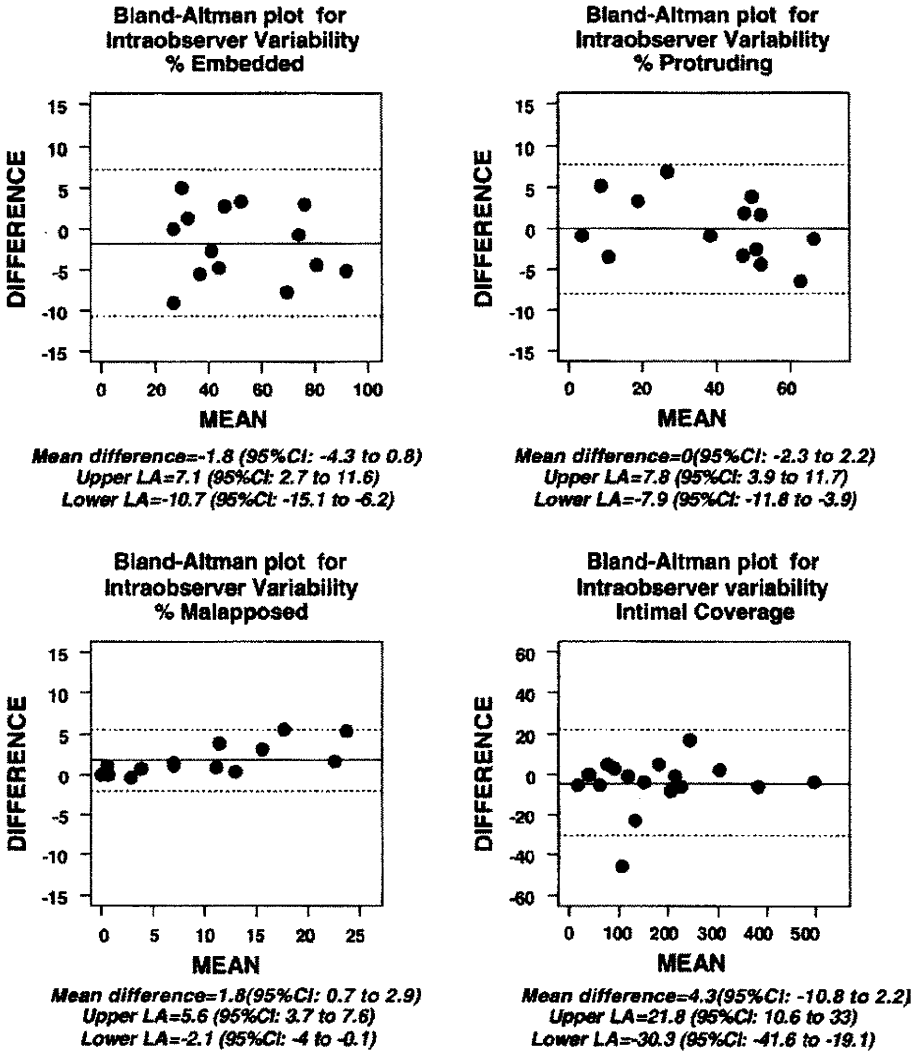

Fig. 2. Bland-Altman plots of intraobserver variability.

strut must also be taken into account (including the metal and polymer thickness) when assessing the distance between the strut and the intima. Moreover, position of the intima behind the strut of interest must be deduced from the adjacent intimal border, which is shadow-free. Despite these limitations of OCT, the low inter and intra observer variability found in this study reflects the high definition of this technology for microstructures such as stent struts.

The classification of strut apposition used in this study was previously proposed by our group [9] (Fig. 1). The rationale of this classification into "embedded", "protruding" and "malapposed" derives from the concept that struts buried into the intima (embedded) have a lower % exposed surface to flow and a higher probability of being covered by the intima in a timely fashion. Protruding struts, although in contact with the intima, have a higher % of exposed surface area to blood, which may affect local flow dynamics and potentially lead to delayed tissue coverage. Malapposed struts are not in contact with the intima, with 100% of their surface exposed to blood flow, possibly resulting in very delayed or no intimal coverage. This may have a bearing both on short and long-term risk of stent thrombosis, given

Table 2
Reproducibility coefficient and intraclass correlation coefficient (expressed as %).

	Reproducibility coefficient	ICC	95%CI
Acute strut apposition			
Intra-observer			
Embedded	9.2%	97.8%	93.5 – 99.2%
Protruding	7.5%	98.4%	95.2 – 99.4%
Malapposed	5.1%	94.9%	85.5 – 98.3%
Inter-observer			
Embedded	10.8%	98.3%	95.1 – 99.4%
Protruding	8.6%	97.3%	92.2 – 99.1%
Malapposed	6.6%	91.3%	75.8 – 97.0%
Neointimal tissue coverage			
Intra-observer	26.7 μm	99.4%	98.6 – 99.8%
Inter-observer	24.1 μm	99.6%	98.8 – 99.8%

ICC-intraclass coefficient, CI-confidence interval.

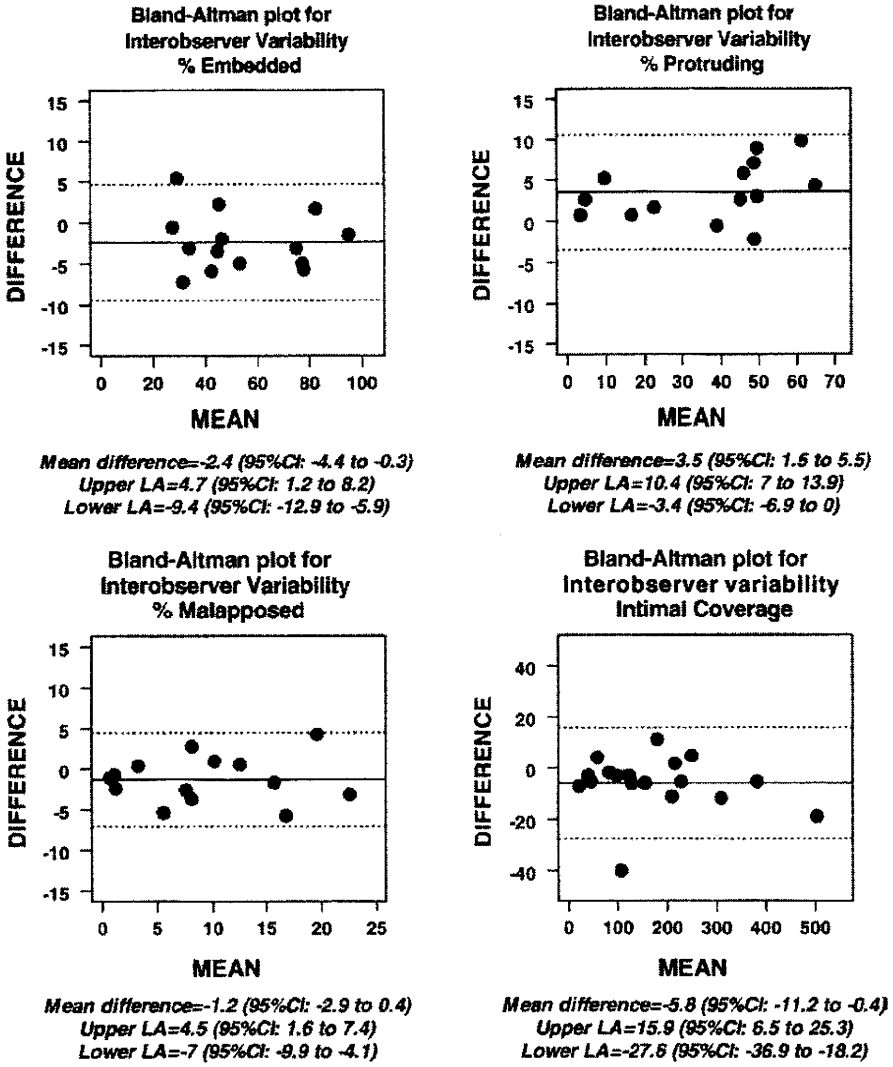

Fig. 3. Bland-Altman plots of interobserver variability.

that post-mortem studies have shown a clear link between malapposed struts, lack of tissue coverage and stent thrombosis [15,17]. This study showed a very high degree of inter and intraobserver agreement using the above classification. Serial OCT studies with long-term follow-up are needed demonstrate the clinical relevance of acute strut apposition classified in this manner.

3.2. Stent strut tissue coverage

OCT is likely to become the new gold standard for assessing stent tissue coverage in-vivo. Several studies have recently been published highlighting the application of OCT in the detection of stent tissue coverage at follow-up. Matsumoto et al. [18] studied 34 patients following sirolimus-eluting stent (SES) implantation. The mean neointima thickness was 52.5 μm. We found comparable intra and interobserver variability to Matsumoto et al., despite a much higher mean neointimal thickness (170 in our study versus 52), likely due to the use of different stent types. The low variability is reassuring, given the potential application and importance of tissue coverage to the clinical setting, with studies having found a link between delayed or incomplete endothelialization and stent thrombosis [19,20].

3.3. Clinical implications

When considering the valuable information gained from OCT, in particular its ability to detect minute tissue coverage over stent struts in-vivo, the intense interest now shown in this field is understandable. OCT is fast becoming an integral component of large clinical stent trials in an attempt to assess tissue coverage and possibly address the incidence of incomplete stent endothelialization in different stent types. Knowledge of intra and interobserver variability of OCT measurements is essential when designing such trials and

when considering OCT findings as a surrogate marker of possible late thrombosis.

3.4. Limitations

Even though our study included a limited number of patients, a very large number of struts were examined using a highly sensitive imaging modality, resulting in very small intra and interobserver variability. Given the relatively recent introduction of OCT for the coronary circulation, only one system with its proprietary analysis software is currently available. Measurements of apposition and intimal tissue are currently performed manually, and are thus extremely time-consuming. In the near future, developments in analysis and data systems will see the extension of IVUS based analysis packages to OCT data. New semi-automated or automated software will be developed and will need to be validated against the current proprietary software. Furthermore, until a precise threshold for the percentage of struts malapposed within a stent is defined by large series of patients undergoing serial OCT, the clinical relevance of the intra and interobserver variability found in our study will remain unclear. Regardless, a high degree of intra and interobserver agreement was present for all measures of apposition.

4. Conclusions

Low intra and interobserver variability can be expected when analyzing intracoronary derived OCT data for stent strut apposition and intimal coverage. This supports the validity of OCT as a clinical and research tool in the setting of intracoronary stent imaging.

Acknowledgement

The authors of this manuscript have certified that they comply with the Principles of Ethical Publishing in the International Journal of Cardiology [21].

References

[1] Tanigawa J, Barlis P, Dimopoulos K, Di Mario C. Optical coherence tomography to assess malapposition in overlapping drug-eluting stents. EuroIntervention 2008;3:580–3.
[2] Takano M, Inami S, Jang IK, et al. Evaluation by optical coherence tomography of neointimal coverage of sirolimus-eluting stent three months after implantation. Am J Cardiol 2007;99:1033–8.
[3] Raffel OC, Tearney GJ, Gauthier DD, Halpern EF, Bouma BE, Jang IK. Relationship between a systemic inflammatory marker, plaque inflammation, and plaque characteristics determined by intravascular optical coherence tomography. Arterioscler Thromb Vasc Biol 2007;27:1820–7.
[4] Kubo T, Imanishi T, Takarada S, et al. Assessment of culprit lesion morphology in acute myocardial infarction: ability of optical coherence tomography compared with intravascular ultrasound and coronary angioscopy. J Am Coll Cardiol 2007;50:933–9.
[5] Tearney GJ, Jang IK, Bouma BE. Optical coherence tomography for imaging the vulnerable plaque. J Biomed Opt 2006;11:021002.
[6] Jang IK, Tearney GJ, MacNeill B, et al. In vivo characterization of coronary atherosclerotic plaque by use of optical coherence tomography. Circulation 2005;111:1551–5.
[7] Tearney GJ, Yabushita H, Houser SL, et al. Quantification of macrophage content in atherosclerotic plaques by optical coherence tomography. Circulation 2003;107:113–9.
[8] Barlis P, Tanigawa J, Di Mario C. Coronary bioabsorbable magnesium stent: 15-month intravascular ultrasound and optical coherence tomography findings. Eur Heart J 2007;28:2319.
[9] Tanigawa J, Barlis P, Di Mario C. Intravascular optical coherence tomography: optimisation of image acquisition and quantitative assessment of stent strut apposition. EuroIntervention 2007;3:128–36.
[10] Tanimoto S, Rodriguez-Granillo G, Barlis P, et al. A novel approach for quantitative analysis of intracoronary optical coherence tomography: high inter-observer agreement with computer-assisted contour detection. Catheter Cardiovasc Interv 2008;72:228–35.
[11] Bland JM, Altman DG. Statistical methods for assessing agreement between two methods of clinical measurement. Lancet 1986;1:307–10.
[12] Tanabe K, Serruys PW, Degertekin M, et al. Incomplete stent apposition after implantation of paclitaxel-eluting stents or bare metal stents: insights from the randomized TAXUS II trial. Circulation 2005;111:900–5.
[13] Hong MK, Mintz GS, Lee CW, et al. Late stent malapposition after drug-eluting stent implantation: an intravascular ultrasound analysis with long-term follow-up. Circulation 2006;113:414–9.
[14] Fujii K, Carlier SG, Mintz GS, et al. Stent underexpansion and residual reference segment stenosis are related to stent thrombosis after sirolimus-eluting stent implantation: an intravascular ultrasound study. J Am Coll Cardiol 2005;45:995–8.
[15] Cook S, Wenaweser P, Togni M, et al. Incomplete stent apposition and very late stent thrombosis after drug-eluting stent implantation. Circulation 2007;115:2426–34.
[16] Uren NG, Schwarzacher SP, Metz JA, et al. Predictors and outcomes of stent thrombosis: an intravascular ultrasound registry. Eur Heart J 2002;23:124–32.
[17] Joner M, Finn AV, Farb A, et al. Pathology of drug-eluting stents in humans: delayed healing and late thrombotic risk. J Am Coll Cardiol 2006;48:193–202.
[18] Matsumoto D, Shite J, Shinke T, et al. Neointimal coverage of sirolimus-eluting stents at 6-month follow-up: evaluated by optical coherence tomography. Eur Heart J 2007;28:961–7.
[19] Bouma BE, Tearney GJ, Yabushita H, et al. Evaluation of intracoronary stenting by intravascular optical coherence tomography. Heart 2003;89:317–20.
[20] Diaz-Sandoval LJ, Bouma BE, Tearney GJ, Jang IK. Optical coherence tomography as a tool for percutaneous coronary interventions. Catheter Cardiovasc Interv 2005;65:492–6.
[21] Coats AJ. Ethical authorship and publishing. Int J Cardiol 2009;131:149–50.

INTERNAL MEDICINE

□ CASE REPORT □

Rapidly Progressing Aneurysm of Infected Thoracic Aorta with Pseudoaneurysm Formation

Akio Iimori[1], Yumiko Kanzaki[1], Shinpei Ito[2], Takuya Kotani[3], Suzue Hirano-Kuwata[3], Masahiro Daimon[4], Takahiro Katsumata[4], Hiroyuki Akagi[5], Tsuyoshi Komori[5], Fumio Terasaki[1], Nobukazu Ishizaka[1] and Akira Ukimura[2]

Abstract

A 60-year-old man presented with chest discomfort with fever and high C-reactive protein (CRP). Chest computed tomography (CT) disclosed a mediastinal soft tissue swelling originating from the aortic arch, and gallium-67 single-photon emission CT revealed intense uptake in the same region. We initially suspected mediastinitis and/or a thoracic aortic infection. Antibiotics improved his symptoms and CRP levels. However, a follow-up CT scan 33 days later, revealed an aortic arch aneurysm and the patient was diagnosed with infective aortic aneurysm. Here, we report a rare case of a rapidly progressing aneurysm of infected aorta aortic infection with pseudoaneurysm formation.

Key words: infected aneurysm, gallium scintigraphy, computed tomography, SPECT/CT

(Intern Med 49: 2461-2465, 2010)
(DOI: 10.2169/internalmedicine.49.4068)

Introduction

Infection of the aorta is rare and difficult to treat, and it is associated with significant mortality. The key to survival is early diagnosis followed by intensive treatment with appropriate antibiotics and prompt surgical intervention. An immediate diagnosis should be pursued based on computed tomography (CT). Fusion images obtained from CT and gallium-67 citrate (Ga-67) single-photon emission CT (SPECT) are also useful in confirming the location of an infected aorta. Here, we present a rare case of a rapidly progressing aneurysm of infected thoracic aorta associated with pseudoaneurysm formation.

Case Report

A 60-year-old man with diabetes mellitus, hypertension, and a history of radiation therapy for laryngeal cancer was admitted initially to another hospital because of chest pain, high fever of unknown origin, and high C-reactive protein (CRP) concentration. Despite a few days of intravenous antibiotic treatment for the bacterial infection with unknown foci, the fever and CRP concentration remained unchanged. Owing to persistent fever, the patient was referred to our institution for further evaluation and treatment. On admission, he complained of having had chest discomfort during the preceding week. On initial examination, his body temperature was 38.3℃, blood pressure was 166/87 mmHg, his heart rate was 110 beats/min, and respiratory rate was 28 breaths/min. The oxygen saturation was 98%. Physical examinations revealed no remarkable signs. A chest radiograph revealed a mild widening of the mediastinum (Fig. 1) and an electrocardiogram showed sinus tachycardia and left ventricular hypertrophy. Laboratory studies, summarized in Table 1, revealed leukocytosis with a white blood cell (WBC) count of 13,390 cells/μL (91% neutrophils, 3% lymphocytes, and 4% monocytes) and a CRP concentration of 30.7 mg/L. Chest CT disclosed a mediastinal soft tissue swelling originating from the aortic arch with upper mediastinitis

[1]Department of Internal Medicine III, Osaka Medical College, Takatsuki, [2]Department of General Medicine, Osaka Medical College, Takatsuki, [3]The First Department of Internal Medicine, Osaka Medical College, Takatsuki, [4]Department of Cardiovascular Surgery, Osaka Medical College, Takatsuki and [5]Department of Radiology, Osaka Medical College, Takatsuki
Received for publication June 11, 2010; Accepted for publication August 20, 2010
Correspondence to Dr. Yumiko Kanzaki, in3089@poh.osaka-med.ac.jp

(Fig. 2A). We suspected mediastinitis and/or thoracic aortic infection as an inflammatory cause. A transthoracic echocardiogram revealed no evidence of infective endocarditis and a gastroscopy revealed no particular finding of mediastinitis. Empirical treatment with ceftriaxone 2 g/day and vancomycin (VCM) 1 g/day and strict control of serum blood sugar level were initiated parenterally. Ga-67 scintigraphy showed abnormal accumulation at the same site. We also performed a Ga-67 SPECT and fused the images with his chest CT images (Fig. 3), which supported the notion that this region was the source of the inflammation. The infectious parameters gradually improved after a few days, and the patient's symptoms also showed improvement. On day 14 of hospitalization, a follow-up chest CT showed that the swelling of the aortic arch had reduced (Fig. 2B). We continued the antibiotics and on day 30, the patient complained of slight back pain. On day 33, follow-up chest CT showed an aortic arch aneurysm that had developed rapidly (Fig. 2C). In addition, magnetic resonance imaging (MRI) showed a saccular aneurysm at the aortic arch (Fig. 4), therefore the patient was diagnosed to have infective aortic arch aneurysm. We tried to conduct strict blood pressure control and continued the antibiotic therapy. We also changed VCM to linezolid as it is thought to have better tissue distribution and is more suitable for patients with renal dysfunction. However, on day 40, another follow-up chest CT revealed the progressive enlargement of the aortic arch aneurysm compared with that observed one week previously (Fig. 2D). We decided to perform immediate surgery when the signs of impending rupture were proven on CT. A preoperative aorta-coronary angiogram showed normal coronary vessels. Thereafter, on day 50, partial aortic arch replacement was performed (Fig. 5). The aneurysm was saccular in shape and had a punched-out orifice, a very thin wall, and a thick mural thrombus, therefore we diagnosed this saccular aneurysm was pseudoaneurysm. During surgery, the infected aortic tissue was debrided, and the infected area was found to be more widespread than that indicated by CT imaging. In addition, a mycotic pseudoaneurysm was also noted in the arch region, because a descending aorta-to-aortic arch prosthetic interposition graft was implanted and connected to the innominate artery smoothly. The patient's blood cultures and resected tissue cultures tested thereafter were negative. A pathological exam revealed an atheroma that had been deposited by cholesterin on an aortic wall. The adventitial site exhibited fibrosis, hyperplasty of small vessels, and neutrophil infiltration, but no bacterial colony was apparent.

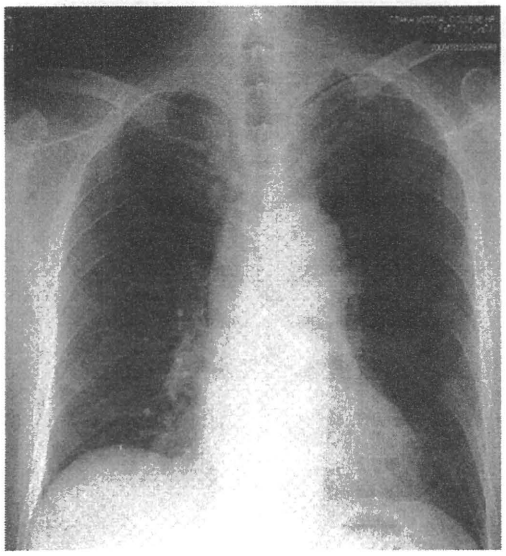

Figure 1. Chest X-ray on admission.

The postoperative course was uneventful. After surgery, antibiotics were administered with ampicillin sodium/sulbactam sodium 3 g/day and linezolid 1,200 mg/day for 3 weeks intravenously, and then linezolid 600 mg/day for 3 weeks orally. The patient's overall condition remained good and he was discharged 44 days after the surgery. He has remained in a stable condition for a year after surgery.

Discussion

Here, we present a case of rapidly progressing aneurysm of infected thoracic aorta with pseudoaneurysm formation, which resolved after intensive antibiotic therapy and surgical therapy. Infected aorta is an uncommon though potentially devastating condition with only 0.7-2.7% of all aortic aneu-

Table 1. Laboratory Findings on Admission

Hematology			Biochemistry		
WBC	13390	cells/μL	AST	65	IU/L
RBC	459	$\times 10^4$ cells/μL	ALT	70	IU/L
Hb	13.5	g/dL	LDH	213	IU/L
Ht	38	%	CK	28	IU/L
Plat	34	$\times 10^4$ platelets/μL	BS	335	mg/dL
			CRP	30.7	mg/dL
			Cre	0.9	mg/dL
Blood culture	(-)		BUN	14	mg/dL
			UA	14	mg/dL
			T-Cho	211	mg/dL
			Na	132	mEq/L
			K	4.2	mEq/L
			Cl	94	mEq/L
			HbA1C	11.3	%